




Article

Degradation and In Vivo Response of Hydroxyapatite-Coated Mg Alloy

Yevheniia Husak ¹, Oleksandr Solodovnyk ¹, Anna Yanovska ² , Yevhenii Kozik ¹, Iryna Liubchak ¹, Viktoriia Ivchenko ³ , Oleg Mishchenko ⁴, Yevhen Zinchenko ⁵, Vladimir Kuznetsov ⁵ and Maksym Pogorielov ^{1,*} 

¹ Medical Institute, Sumy State University, 2 R-Korsakova Str, 40007 Sumy, Ukraine; evgenia.husak@gmail.com (Y.H.); dr.solovi@gmail.com (O.S.); yevhenii.kozik@gmail.com (Y.K.); irinalybchak@gmail.com (I.L.)

² Department of General Chemistry, Sumy State University, 2 R-Korsakova Str, 40007 Sumy, Ukraine; yanovskaanna@gmail.com

³ Department of Therapy, Pharmacology, Clinical Diagnostics and Chemistry, Sumy National Agrarian University, 160 H. Kondratiev Str., 40021 Sumy, Ukraine; ivchenkovd@gmail.com

⁴ Osteoplast R & D, 25 Metalowkow Str., 39-200 Debica, Poland; Dr.Mischenko@i.ua

⁵ Institute of Applied Physics, National Academy of Sciences of Ukraine, 58 Petropavlovskaya St., 40030 Sumy, Ukraine; yarabey93@gmail.com (Y.Z.); vldnik84@gmail.com (V.K.)

* Correspondence: m.pogorielov@gmail.com; Tel.: +38-066-900-54-48

Received: 24 June 2018; Accepted: 20 October 2018; Published: 23 October 2018



Abstract: Nowadays there is a need for new generation of biodegradable implants, which should be able to stimulate the healing responses of injured tissues at the molecular level. Magnesium alloys attract great attention as perspective bone implants due to their biocompatibility, physical properties and ability to degrade completely under physiological conditions. The main purpose of this research was assessment of in vitro corrosion and surface morphology after short term in vivo implantation of Mg based implant covered by hydroxyapatite (HA). Mg alloys with the addition of Zr (0.65%), Al (1.85%) and Nd (1.25%) were used. In our work, we propose dipping method for hydroxyapatite coatings formation which has been shown to reduce the corrosion rate of magnesium implants in vivo. Simulated body fluid (SBF; pH 7.4) with ion concentrations approximately equal to those of human blood plasma resembling physiological conditions and citrate buffer with pH 5—simulating inflammation were selected as modelling environments for in vitro degradation test. The rod samples were implanted into the tibia bone of rats and after 1 day and 5 days of implantation were taken out to observe cells adhesion on surface samples. SEM was used to assess surface morphology after in vitro and in vivo tests. SBF solution causes some cracks on the surface of HA coatings, while citrate solution at pH 2 caused complete dissolving of the coating. The HA coating favoured cell adhesion and rapid fibrous tissue formation.

Keywords: Mg alloy; corrosion; HA coating; implantation

1. Introduction

Nowadays trauma and orthopaedic surgery cannot be imagined without biomaterials. Bone substitutes, such as biodegradable polymers, metals, ceramics and bioactive glasses are widely used to facilitate bone fracture healing or to compensate for a lack or loss of bone tissue [1,2]. Among mentioned kinds of materials, magnesium alloys attract great attention as perspective bone implants due to their biocompatibility, physical properties and an ability to biodegradation that eliminates the need of surgical reintervention. First attempts of applying biodegradable Mg alloys as a material for osteosynthesis were made in 1906 by Lambotte and resulted in clinical failure [3,4].

Despite the fact that recently considerable researches were performed for creation an ideal orthopaedic metallic implant, there remain a lot of critical factors to solve in this field.

Mg alloys have a number of advantages before other bone substitutes. Mg is an essential element inside human body: it performs a function of cofactor to many enzymes and stabilization of DNA and RNA structure [2]. It could be safely used as a main compound of orthopaedic implant [5]. Moreover, some researches show that Mg could have stimulatory effects on the formation of new bone [6]. Hence, the main problem of developing advanced Mg alloys for medical application is combining degradation with tissue healing rate. Orthopaedic metallic implants should maintain their mechanical properties for at least 3 months to avoid the second fracture occurrence resulting from their fast degradation [5,7].

Magnesium based alloys possess high specific strength, making them an attractive material for structural applications [8]. Mg alloys have superior mechanical properties: density and Young's modulus (shows an ability to resist deformation) close to those of natural bone if compare they with other metal commercial bone implants [9].

Mg and its alloys have high electronegative potentials and can, therefore, degrade in aqueous solutions via an electrochemical reaction, which produces magnesium hydroxide and hydrogen gas. Under physiological conditions where a high concentration of chlorides exists, Mg alloy shows high degradation rate, because $Mg(OH)_2$ can rapidly convert into highly soluble $MgCl_2$, which increases corrosion of an alloy [9]. Fast and uncontrolled corrosion associated with hydrogen ion release remains a serious problem of Mg alloys degradation [2,3]. Hydrogen gas, which is formed and accumulated within the surrounding tissues during degradation, leads to inflammatory reactions. In general, severe pH and changes in osmotic pressure have negative influence on organism. In addition, fast resorption of metal implant can lead to mechanical instability before bone healing is completed [2,3,7,10].

The unique corrosion properties of Mg implants make them biodegradable body implants for surgeries [11]. The corrosion behaviour of Mg alloys and their biocompatibility is strongly affected by alloying elements. It was found that inclusion of alloying elements such as Al, Mn, Ca, Zn and rare earth elements provides improved corrosion resistance to Mg alloys. The Mg based biodegradable substrates can be divided into four major groups: pure Mg, Al containing alloys (AZ91, AZ31, LAE422, AM60 etc.), Rare earth elements (AE21, WE43 etc.) and Al free alloys (WE43, MgCa0.8, MgZn6 etc.). These alloying elements improve the mechanical and physical properties of Mg alloys for orthopaedic applications by: optimising grain size, improve corrosion resistance, providing mechanical strength by the formation of intermetallic states and eases the manufacture process of Mg alloys. As an alloying element, Al is commonly used for modifying the mechanical and corrosion properties of Mg alloys. Addition of 1%–5% Al leads to the reduction of grain size, it dissolves partly in Mg solid solutions and precipitate as secondary phases that show different electrode potentials.

Rare-earth elements form intermetallic phases with Mg and Al which have a pronounced effect on the strength and corrosion of Mg alloys. Rare-earth-containing alloys show beneficial mechanical properties and excellent creep resistance. Addition of Zr also improves tensile strength, ductility grain refining and corrosion resistance of implant material [12]. Mg–Nd–Zn–Zr alloy has excellent in vitro blood compatibility and thus can be considered as a potential degradable biomaterial for medical applications with respect to hemocompatibility [13]. A direct adhesion experiment showed good cell spreading and adhesion on Mg alloy with Zr, Al and Nd [14].

Many optimization procedures were developed for improvement of Mg alloys corrosion resistance. They include alloy composition design [5,15,16] and surface modifications [2,9,17]. The alloying elements in self-resorbable Mg alloys should be selected not only on the improvement of mechanical properties but also on the consideration of degradation and biocompatibility [1,18]. Currently, a wide range of mechanical, chemical and physical methods are used for surface modification of Mg alloys, including coating creation techniques. It also decreased the mechanical loss at the early stage adapting to the load-bearing requirement at this stage. It improved the bio-adhesion of Mg alloys with the surrounding tissue, which is believed to be contributed to the tissue adaptability of the surface modification. Therefore, the surface modification adapts the biodegradable magnesium

alloys to the need of biodegradation, biocompatibility and mechanical loss property. For the different clinical application, different surface modification methods can be provided to adapt to the clinical requirements for the Mg alloy implants [19] among them are coatings of CrN, TiN, Ti–Al–N, AlN and TiO₂ [20,21] obtained by various techniques, ion implantation [22], alkali-heat-treatment [23] and calcium-phosphate coatings of [24–27].

Hydroxyapatite (Ca₁₀(PO₄)₆(OH)₂) resembles the structure of mineralized bone and therefore, is widely used as the coating of bone implant materials. It has such properties as excellent biocompatibility, nontoxicity, bioactivity, osteoconductivity and thermodynamic stability [28]. But ideal method for Mg–alloy surface coating formation to provide osteointegration and decrease the degradation time is still not found.

The purpose of this research was assessment of in vitro corrosion and surface morphology after short term in vivo implantation of Mg based implant with HA coating.

2. Materials and Methods

2.1. Materials

Mg alloy with the contents of Mg, Al, Zr, Nb (commercially available) are 96.25 wt.%, 1.85 wt.%, 0.65 wt.%, 1.25 wt.%, respectively was obtained from Department of Ceramics, Composites and Foundry Technologies (Politechnika Śląska, Gliwice, Poland). The alloy was produced using pure Mg, Al (99.9% purity) and Al–Zr, Al–Nd master alloys. Melting of the alloys was conducted by induction melting in an Al₂O₃ crucible under the protection of an argon atmosphere. The melt was held at 730 °C for 5 min then poured into sand moulds. Uncoated Mg alloy has flat surface that is presented in the Figure 1.

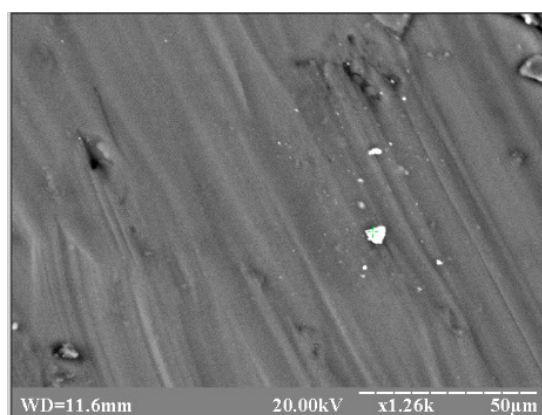


Figure 1. SEM image of surface morphology of uncoated Mg alloy.

All the specimens of Mg alloys have the size of 4 × 1 × 1 mm³ (for in vivo experiments) and 8 × 1 × 1 mm³ (for in vitro experiments). Hydroxyapatite coatings were used to improve the corrosion resistance of magnesium and its alloys as well as their surface bioactivity.

Dipping method was provided in this work for coating deposition. Solutions of 0.1 M CaCl₂ and 0.06 M Na₂HPO₄ were prepared by dissolving 11.1 g and 8.52 g in 1 L of double distilled water respectively. Then equal volumes of initial solutions were mixed in relation 1:1. For coating deposition 200 mL of obtained solution was taken. Mg substrates were cleaned by sequential triple washing in acetone and 96% ethanol solutions. All samples were immersed into 200 mL of initial Ca–P solution without polishing with exception of Samples (b) and (f) that were polished with sandpaper P240 (according to ISO/FEPA designation) with average particle diameter 58.5 µm. Obtaining of hydroxyapatite coatings by dipping method were provided without agitation at various time periods from 0.5 to 48 h and conditions given in the Table 1. Thermostat was used to maintain temperature of deposition at constant level 30 and 50 °C. Room temperature 22 °C was measured during experiment by

thermometer. Basic pH was obtained due to partial corrosion of Mg-alloy substrates during immersion in initial solution as well as rough surface which is necessary for better coating adhesion.

Table 1. Experimental conditions of HA coatings deposition on Mg-alloy substrates by dipping method.

| Sample Number | Experimental Conditions |
|---------------|-------------------------|
| (a) | 24 h, 22 °C |
| (b) | 24 h, 22 °C, polished |
| (c) | 48 h, 22 °C |
| (d) | 2 h, 22 °C |
| (e) | 1 h, 30 °C |
| (f) | 1 h, 50 °C, polished |
| (g) | 1 h, $t = 50$ °C |
| (h) | 0.5 h, $t = 30$ °C |
| (i) | 1.5 h, $t = 30$ °C |

Physical adhesion contributes to the interatomic attraction within the material. Thus, for maximum adhesion of HA coatings the quality of the surface to be coated is of critical importance. In particular, the activation of the substrate must guarantee good mechanical anchorage. Surface preparation is necessary to ensure adequate adhesion to the substrate. This is achieved via surface activation that comprises three stages: degree of cleanliness, surface roughness and surface microstructure. For this purpose, Samples (b) and (f) were polished with sandpaper [29]. Experimental conditions are described in the (Table 1).

Simulated body fluid (SBF; pH 7.4) with ion concentrations approximately equal to those of human blood plasma resembling physiological conditions and citrate buffer solutions with pH 5 and pH 2 simulating inflammation and acidic surroundings were selected as modelling environments.

In the present study triplicate trials were performed for each experiment. The mean values and standard deviation were calculated from obtained data.

2.2. In Vitro Degradation

To examine the in vitro degradation behaviour of the HA-coated and uncoated Mg alloy samples, the samples with the size of $8 \times 1 \times 1$ mm³ were immersed in SBF solution for different time and the pH values of the SBF were monitored every day during the immersion test. SBF solution was refreshed every 24 h.

The in vitro response of the coatings was studied by immersing the uncoated and HA-coated substrates (e), (h) and (i) in 50 mL of SBF (pH = 7.40) for 7 days at 37 °C. SBF solution was prepared according to the Table 2. Volume 50 mL is enough for accurate measuring of pH during degradation. SBF solutions were renewed every 24 h to ensure constant initial chemical composition. pH of solutions was measured by using pH meter before refreshing of SBF solutions. After being soaked for 7 days, the specimens were washed with distilled water and then dried at room temperature for 24 h. Citrate buffer solution with pH = 5 was used for modelling of inflammation process in bone tissue. It was prepared by dissolving of 20.5 mL of 0.1 M citric acid: 19.21 g/L (M.W.: 192.1) and 29.5 mL of 0.1 M sodium citrate dihydrate: 29.4 g/L (M.W.: 294.0) in 100 mL of distilled water to obtain pH = 5. Buffer solution with pH = 2 used for modelling of acidic conditions. It was prepared by adding 46.5 mL of 0.1 M citric acid and 3.5 mL of 0.1 M sodium citrate dihydrate in 100 mL of deionized water. pH was adjusted to 2 by titration with 0.1 M HCl solution [30].

Table 2. Reagents used to prepare 1 L of the SBF solution (pH = 7.40) [31].

| Oder | Reagent | Amount |
|------|--|-------------------------------------|
| 1 | NaCl | 7.996 g/L |
| 2 | NaHCO ₃ | 0.350 g/L |
| 3 | KCl | 0.224 g/L |
| 4 | K ₂ HPO ₄ ·3H ₂ O | 0.228 g/L |
| 5 | MgCl ₂ ·6H ₂ O | 0.305 g/L |
| 6 | 1 kmol/m ³ HCl | 40 cm ³ |
| 7 | CaCl ₂ | 0.278 g/L |
| 8 | Na ₂ SO ₄ | 0.071 g/L |
| 9 | (CH ₂ OH) ₃ CNH ₂ | 6.057 g/L |
| 10 | 1 kmol/m ³ HCl | Appropriate amount for adjusting pH |

2.3. In Vivo Test

12 male rats were involved in experiment and randomized in two groups—pure Mg Alloy with the size of $4 \times 1 \times 1 \text{ mm}^3$ and HA-coated Mg alloy. Housing of the animals and all experimental procedures were carried in accordance with the European Convention for the Protection of Vertebrate Animals used for Experimental and Other Scientific Purposes (Strasbourg, 1986); Directive 2010/63/EU of the European Parliament and of the Council of 22 September 2010 on the Protection of Animals Used for Scientific Purposes. The procedures were approved by the Institutional Ethic Committee (Sumy State University).

The samples were sterilized with 70% ethanol during 2 h and dried under UV irradiation (UV-STERILIZER 8 W, Ultra-Violet Products Ltd., Upland, CA, USA).

Under general anaesthesia (Ketamine 7 mg/kg) was performed implantation of cylindrical rods in middle part of tibia. After 1 day and 5 days of experiment, animal implants were taken out to observe cells adhesion on surface samples. Mg rods were in 0.1 mm less compare the implanted cite. Time period 1 day and 5 days are not enough for bone or connective tissue formation. And al rods were easily removed from operation cite.

The cells adhesion on the samples was observed using REMMA-102 (SELMi, Sumy, Ukraine) after 1 day and 5 days in vivo experiments. Prior to the observation, the cells on the samples were fixed with 2.5% glutaraldehyde for 10 min, dehydrated in graded ethanol 70%, 90%, 95% and 100% ethanol in sequence and then dried in air.

2.4. Material Characterization

Surface morphology of Mg implants with HA coatings and cell adhesion were evaluated by using of scanning electronic microscopy REMMA102 (SELMi, Sumy, Ukraine) and REM 106 (SELMi, Sumy, Ukraine). To avoid surface charge accumulation, samples were covered with thin (30–50 nm) layer of silver in the vacuum set-up VUP-5M (SELMi, Sumy, Ukraine).

The phase composition of the obtained coatings was examined using an X-ray diffractometer DRON-4-07 (Burevestnik, St. Petersburg, Russia) connected to a computer-aided system for the experiment control and data processing. The Ni-filtered Cu K α_2 radiation (wavelength 0.154 nm) with a conventional Bragg-Brentano θ – 2θ geometry was used. The current and the voltage of the X-ray tube were 20 mA and 40 kV, respectively. The samples were measured in the continuous registration mode at a rate of 2°/min, with 2θ -angles ranging from 15° to 55°. All experimental data were processed with the program package DIFWIN-1 (Etalon PTC, Moscow, Russia). Phase identification was performed using a JCPDS (Joint Committee on Powder Diffraction Standards) card catalogue. After in vivo test samples were fixed in 2.5% glutaraldehyde solution for 24 h, then washed with distilled water and dehydrated in ethanol series with increasing concentrations (35%, 50%, 70%, 80%, 95% \times 2 times, 100%). After drying in desiccators under room temperature samples morphology was investigated by SEM (REMMA102, SELMi, Sumy, Ukraine). Relation of Ca/P were calculated from the results of EDX analysis on REMMA102 (SELMi, Sumy, Ukraine).

3. Results and Discussion

3.1. Samples Characterization

Surface morphologies of coatings obtained on Mg alloy substrates strongly depend on experimental conditions: deposition time and temperature. Immersion of Mg alloy substrates in Ca–P solution at 22 °C for 24 and 48 h did not provide formation of uniform coating (Figure 2b–d). Thickness of obtained coatings is 0.2–0.5 µm. In the case of uniform coating we can observe cracks formation that can affect degradation of implant during in vivo tests (Figure 2a). The coatings obtained at room temperature (22 °C) need enough time for crystallization so they are more uniform after 24–48 h of crystallization. At 50 °C fast coating formation was observed, besides the corrosion rate was also increased (Figure 2f–g). At 30 °C, the obtained coatings were the most uniform (Figure 2e–i). Coatings of HA (Figure 2f–i) have developed surface morphology that could be favourable during in vitro degradation test.

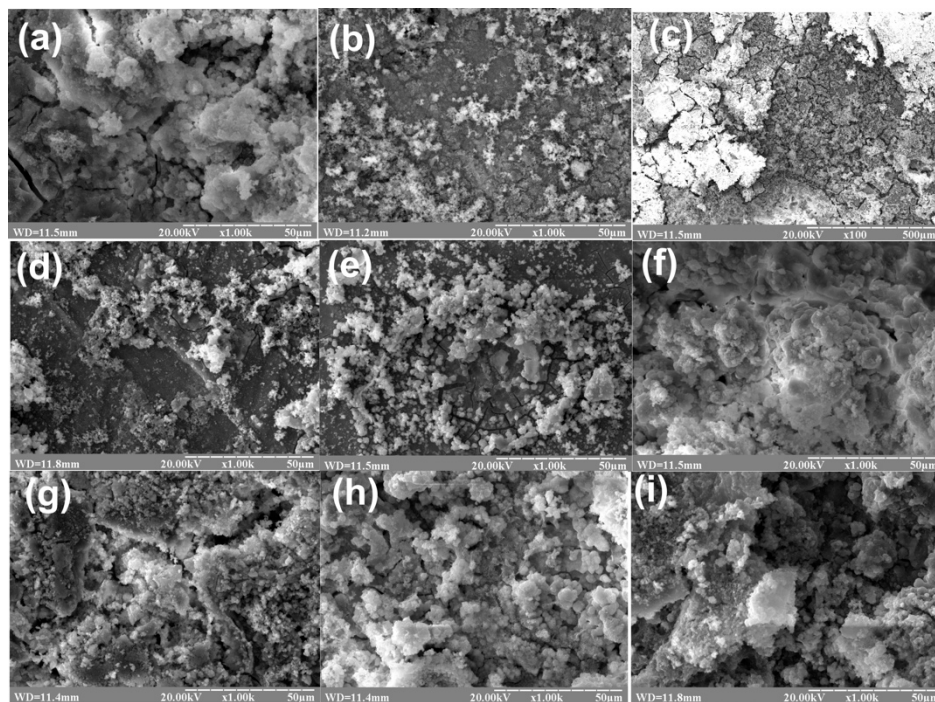


Figure 2. SEM images of surface morphology of HA coatings on Mg substrates deposited under following conditions: (a) 24 h, 22 °C; (b) 24 h, 22 °C, polished; (c) 48 h, 22 °C; (d) 2 h, 22 °C; (e) 1 h, 30 °C; (f) 1 h, 50 °C, polished; (g) 1 h, $t = 50$ °C; (h) 0.5 h, $t = 30$ °C; (i) 1.5 h, $t = 30$ °C.

Temperature is the main factor of HA coating formation on Mg alloy. Feng et al. [32] carried out deposition of HA at 80 °C in a water bath for 20 min. In other research HA coatings on Mg alloys were deposited for 6 h at 95 °C [33]. Coatings obtained in both experiments present excellent biological activity and high corrosion resistance. On the other hand, Zhang et al. [34] used HA powder in 0.70 wt.% phytic acid solution to obtain coating on AZ31 magnesium alloy at 40 °C for 20 min. They did not observe uniform layers and presence of cracks. So, in these experiments we draw a conclusion that it would be better to reduce time and increase temperature during HA coating deposition onto Mg substrate.

The elemental composition of the coatings was examined by EDX attached to SEM (Figure 3) and results show that the coatings mainly contain Ca and P elements. The Ca/P atomic ratios of coatings were calculated from EDX analysis results and were for Samples (a)–(d) from 1.52 to 1.62, (e) 1.64 and for Samples (f)–(i) they were 1.66–1.67 that corresponded to stoichiometric HA (1.67). For Samples (a)–(d) we can see that certain degree of calcium deficiency in HA nanocrystals was obtained in these

coatings. As well as EDX results for all samples were completely the same, the EDX spectrum for Sample (i) is presented below:

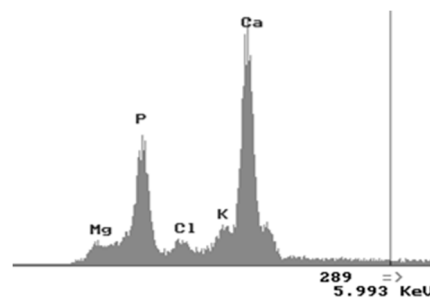


Figure 3. EDX spectra of HA coated Mg Sample (i).

A qualitative phase analysis by X-ray diffraction (Figure 4) shows the presence of the single phase of hydroxyapatite (JCPDS 9-432) with different degrees of crystallinity due to the various synthesis conditions.

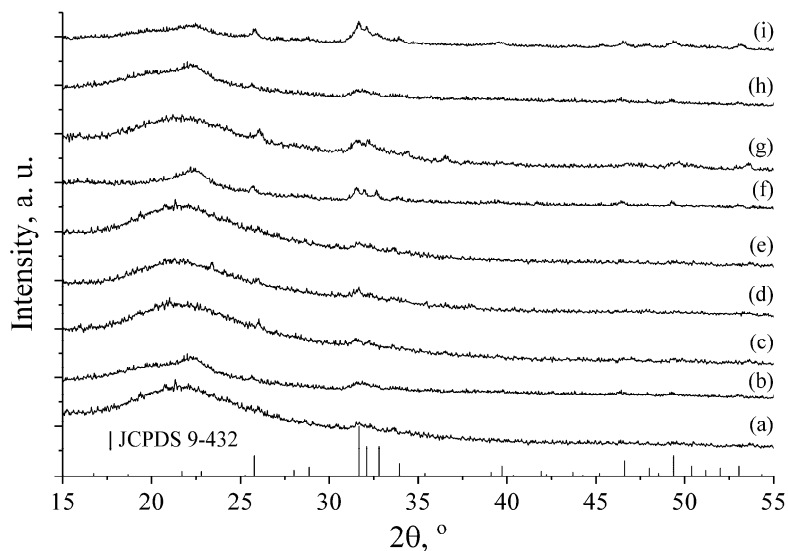


Figure 4. X-ray diffraction patterns of HA coatings on Mg substrates deposited under following conditions: (a) 24 h, 22 °C; (b) 24 h, 22 °C, polished; (c) 48 h, 22 °C; (d) 2 h, 22 °C; (e) 1 h, 30 °C; (f) 1 h, 50 °C, polished; (g) 1 h, $t = 50$ °C; (h) 0.5 h, $t = 30$ °C; (i) 1.5 h, $t = 30$ °C.

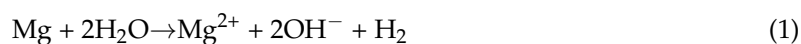
XRD patterns of Samples (a)–(e) show that the crystallinity of HA is lower than for the Samples (f) and (g) obtained at higher temperatures (50 °C). The poor crystallinity of the samples does not allow any additional XRD analysis, except the qualitative one. This analysis clearly shows presence of the HA phase due to the availability of its major peaks: (002) at $2\theta \sim 26^\circ$ and the superposition of (211), (112) and (300) at $2\theta \sim 32^\circ\text{--}33^\circ$. These results are also confirmed by EDX analysis providing Ca/P ratio close to the apatite one.

Formation of HA with higher crystallinity of Sample (i) at 30 °C could be explained by the increase of deposition time to 1.5 h. Peak intensities of HA are very low due to thin apatite coating layer on the Mg alloy. The existence of amorphous halo at $\sim 22^\circ$ 2θ can be explained by the small amount of the samples, which could not cover the significant amount of the cuvette surface used as a sample holder in the X-ray diffractometer.

3.2. In Vitro Degradation Test

Based on SEM results, Sample (f)–(i) were selected for in vitro degradation test. Such samples were more uniform with thicker HA coating without cracks, therefore they were taken for following experiments.

The degradation mechanism of magnesium in aqueous solution can be presented as the following overall reaction [35,36]:



It includes following electrochemical reactions:



Mg undergoes an anodic Equation (1) first. The emitted electrons then participate in a breaking of a water molecule in Equation (2). Equation (3) is the formation of the main corrosion product, magnesium hydroxide $\text{Mg}(\text{OH})_2$, which accumulates on the surface of the Mg matrix.

Degradation products: Mg^{2+} , OH^- and H_2 that were generated from degrading Mg created the microenvironment of bone tissue surrounding of the implants [36]. Anions of OH^- , can directly affect the pH value of the surrounding microenvironment, therefore the pH values were measured during the long-term Mg alloy degradation process. The results showed clearly that the pH values of Mg alloy rose significantly compared to that with HA coatings (Table 3).

$\text{Mg}(\text{OH})_2$ has very low solubility in water, hence its layer on the Mg surface protects it from further degradation [35]. Presence of chloride ions Cl^- in human blood results in conversion of the magnesium hydroxide to magnesium chloride [37], according to the following reaction:



MgCl_2 has much greater solubility in water than $\text{Mg}(\text{OH})_2$. Therefore, MgCl_2 cannot provide an effective protection from corrosion and the magnesium matrix becomes exposed to the aggressive environment again [36]. The corrosion rate of Mg-based implants is a function of several factors: alloying and impurity contents, surface coatings and solution composition [37].

Corrosion of pure Mg and single-phase Mg alloys takes a form of a localized, irregular pitting, which then spreads laterally covering the whole exposed surface. Unlike in stainless steel, heavy pitting does not seem to be present. This is attributed to the fact, that the local increase in pH on the surface of the Mg matrix increases the stability of the protective $\text{Mg}(\text{OH})_2$ film [36].

Presence of an additional phase in the Mg alloy is believed to have two effects on the corrosion behaviour. In case of Rare Earth, the additional phase exhibits a passive corrosion behaviour due to more positive potential than Mg it serves as a cathode for micro galvanic corrosion, thus enhancing the corrosion rate [36].

The minimal change of pH values was observed for Sample (i) 7.49 ± 0.20 and 5.24 ± 0.10 .

Table 3. PH measurements after 24 h for 7 days immersion in SBF solution (average results).

| Sample Number/Initial pH | pH 7.4 | pH 5 | pH 2 |
|--------------------------|-----------------|-----------------|-----------------|
| Mg-alloy | 8.47 ± 0.25 | 5.77 ± 0.58 | 3.25 ± 0.14 |
| (f) | 8.01 ± 0.15 | 5.29 ± 0.11 | 2.59 ± 0.04 |
| (h) | 7.74 ± 0.11 | 5.27 ± 0.13 | 2.59 ± 0.06 |
| (i) | 7.49 ± 0.20 | 5.24 ± 0.10 | 2.57 ± 0.02 |

Table 3 shows the variation of the pH value of SBF solution at different immersion time. The corrosion rate of Mg alloys during the early stages of implantation plays a critical role in the initial surrounding tissue response. The untreated Mg alloy showed a higher pH increase compared to the HA coating specimens. The pH value increases sharply for uncoated sample because of the increase of OH^- concentration caused by the release of Mg^{2+} . The pH for the uncoated sample increases from 7.4 to 8.47 while the pH of coated samples increases only from 0.09 to 0.49. Therefore, it can be concluded that the samples coated with HA have a better corrosion resistance than uncoated sample. In addition, it was observed that the sample (i) coated gave the smallest pH change during 24 h immersion test. This indicates that this sample has the highest corrosion resistance in the present immersion test in SBF solution.

Two samples were chosen for further study: Sample (i) due to the minimal changes in pH values and Mg-alloy as control sample.

After immersion in SBF solution for 24 h the surface of Mg-alloy samples was rough with crackles due to fast degradation of substrate. For the HA coated Sample (i), at pH = 7.40 the surface was more uniform (Figure 5).

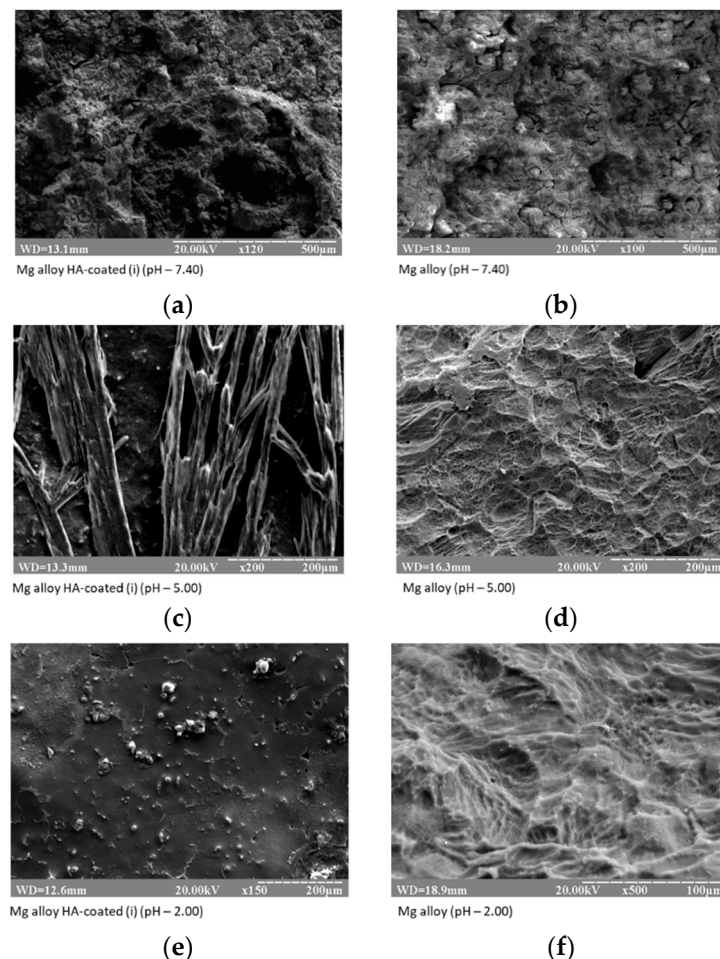


Figure 5. SEM images of the surface of HA–Mg coatings (a,c,e) and Mg–alloys without coatings (b,d,f) after degradation test for 24 h in SBF (pH = 7.40) and in citrate solution (pH = 5.00 and pH = 2.00).

After immersion into citrate solution with pH 5 for 24 h, HA coated Sample (i) was covered by the typical needle-like HA crystals while Mg alloy samples had cellular-like structure. After immersion into citrate buffer with pH = 2 for 24 h a top surface of the coating was dissolved. The surface becomes smooth with some single crystals. In the case of Mg alloy sample citrate solution formed micro points cell cluster structure with higher ridges on its surface.

3.3. In Vivo Test

On first day after implantation the surface structure of Mg-alloy samples have changed. The surface of uncoated implant was covered with small crack network structure, which proved degradation due to the corrosion. Fast degradation impaired mechanical parameters and leads to overproduction of hydrogen gas. At the same time, HA-coated alloy has shown smooth surface with absence of cracks (Figure 6).

It is believed that in a dynamic in vivo environment, the pH in the implanted area associated with a Mg alloy implant would not fluctuate as significantly as in an in vitro environment. However, there would still be a marked increase in pH at the surface of the material in vitro that would also occur in an in vivo environment. HA coatings on Mg alloy surface should mask the negative effect of the pH change associated with Mg corrosion [38].

The positive effect of inorganic coating structure was clearly demonstrated in the Figure 6. Moreover, the biological responses, including cell attachment, proliferation and differentiation, of the HA-coated samples were enhanced considerably compared with the pure magnesium. The reaction of bone tissue to a Mg HA-coated implant showed lack of necrosis and the infiltration of macrophages [39].

In 5 days after implantation, cell adhesion was detected by SEM analysis. Cells were embedded with whitening fibres and distributed on the implant surface. In five days after implantation samples were coated by several layers of connective tissue. But, surface of uncoated implants has numerous cracks that decreased cell adhesion. Cells were randomly attached to uncoated implants. Fast degradation and hydrogen evolution can affect protein adsorption and cell adhesion to uncoated Mg alloy implants.

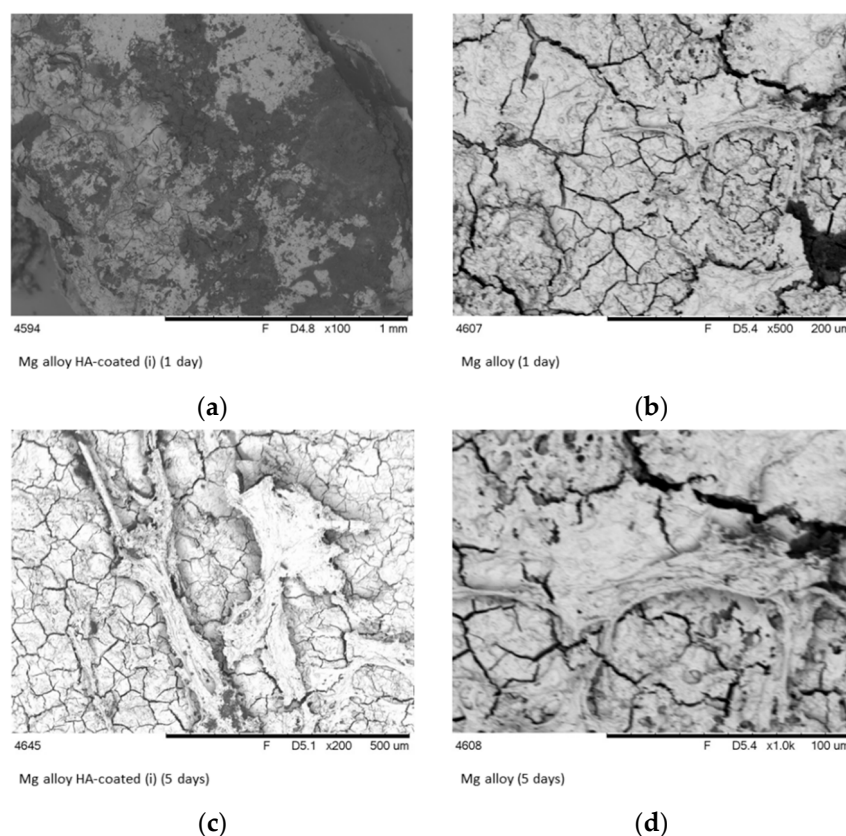


Figure 6. SEM images of the surface of HA-Mg coatings (a,c) and Mg-alloys (b,d) after one and 5 days of implantation in bone tissue.

Low or fast corrosion rate might cause problems during in vitro experiments because gas formation and increase of pH might prevent cell adhesion and proliferation. HA could provide protective layer over metallic surface.

The analysis of the corrosion results exhibits the increase of cell attachment after five days of implantation. The SEM pictures (Figure 6) revealed the differences in the surface appearances and shapes of attached cells between non-coating and HA-coated Mg-alloy. It is predicted that the HA coating of Mg implants will improve the attachment of soft tissue. It is known, that HA is an attractive agent for osteoblast cell line fibroblast-like cells. The adhesion of fibroblasts on implants provides favourable conditions for soft tissue integration. The number of adherent cells on HA-coated Mg-alloy was significantly higher than on the surface of uncoated samples. Two mechanisms can play significant role in cell adhesion: (1) HA coating can prevent following effects, including hydrogen gas cavities, local pH increase and premature mechanical failure [40]; and (2) corrosion resistance can increase cell viability on implant surface.

Large amounts of hydrogen gas and alkalization of the body fluid which, in turn, can inhibit wound healing and ultimately lead to necrosis of the surrounding tissue. In low quantities, these corrosion products can be metabolized in vivo. Thus, reducing the corrosion rate of Mg alloys is required if they are used as implant materials. The corrosion rate directly after implantation is important to allow tissue healing to occur and therefore it is crucial to control the surface degradation of Mg implants after their implantation in vivo.

HA coating layer provides the corrosion resistance of Mg-based alloys. Consequently, local accumulation of hydrogen and fast increase of local pH value are reduced as evidenced by insignificant changes of pH in model solutions.

4. Conclusions

In our work we propose simple, fast and inexpensive method of HA coatings formation on Mg alloy that can be used as medical implant material. This step was taken to reduce pH increase in the place of implantation and protect implant material from corrosion in cell culture environment. Dipping method can provide uniform HA coating on Mg alloy that is strongly depends on temperature. With increasing temperature to 50 °C, the obtained HA coatings were more uniform without cracks and have shown better results compared with coatings obtained at the room temperature. After immersion in SBF solution the surface of Mg-alloy samples was rough with crackles due to fast degradation of substrate. For the HA coated Sample (i) obtained at 50 °C, the surface was more uniform. After immersion into citrate solution with pH 5, HA coated Sample (i) was covered by the typical needle-like HA crystals, while Mg alloy samples had cellular-like structure. After immersion into citrate buffer with pH = 2 a top surface of the coating was dissolved. In the case of Mg alloy sample citrate solution formed micro points cell cluster structure with higher ridges on its surface. HA coating decreased degradation of Mg alloy substrates and pH changes that leads to favoured cell adhesion and rapid fibrous tissue formation. The number of adherent cells on HA-coated Mg-alloy was significantly higher than on the surface of uncoated samples.

Author Contributions: Conceptualization, Y.H. and M.P.; Methodology and Software O.S., I.L., Y.K. and V.I.; Investigation and Data Curation, Y.H., A.Y., O.M., Y.Z. and V.K.; Writing—Original Draft Preparation, Y.H. and A.Y.; Writing—Review and Editing and Supervision, M.P.

Funding: This research was funded by H2020 Marie Skłodowska-Curie Actions (NanoSurf 777926).

Conflicts of Interest: The authors declare no conflict of interest.

References

1. Radha, R.; Sreekanth, D. Insight of magnesium alloys and composites for orthopedic implant applications—A review. *J. Magnes. Alloy.* **2017**, *5*, 286–312. [[CrossRef](#)]
2. Li, L.; Zhang, M.; Li, Y.; Zhao, J.; Qin, L.; Lai, Y. Corrosion and biocompatibility improvement of magnesium-based alloys as bone implant materials: A review. *Regen. Biomater.* **2017**, *4*, 129–137. [[CrossRef](#)]
3. Pogorielov, M.; Husak, Y.; Solodovnik, O.; Zhdanov, S. Magnesium-based biodegradable alloys: Degradation, application, and alloying elements. *Int. Med. Appl. Sci.* **2017**, *9*, 27–38. [[CrossRef](#)] [[PubMed](#)]

4. Lambotte, A. L'utilisation du magnésium comme matériel perdu dans l'ostéosynthèse. *Bull. Mem. Soc. Nat. Chir. Paris* **1932**, *28*, 1325–1334.
5. Gu, X.-N.; Zheng, Y.-F. A review on magnesium alloys as biodegradable materials. *Front. Mater. Sci. China* **2010**, *4*, 111–115. [[CrossRef](#)]
6. Zreiqat, H.; Howlett, C.R.; Zannettino, A.; Evans, P.; Schulze-Tanzil, G.; Knabe, C.; Shakibaei, M. Mechanisms of magnesium stimulated adhesion of osteoblastic cells to commonly used orthopaedic implants. *J. Biomed. Mater. Res.* **2002**, *62*, 175–184. [[CrossRef](#)] [[PubMed](#)]
7. Tang, J.; Wang, J.; Xie, X.; Zhang, P.; Lai, Y.; Li, Y.; Qin, L. Surface coating reduces degradation rate of magnesium alloy developed for orthopaedic applications. *J. Orthop. Transl.* **2013**, *1*, 41–48. [[CrossRef](#)]
8. Chu, P.-W.; Le Mire, E.; Marquis, E.A. Microstructure of localized corrosion front on Mg alloys and the relationship with hydrogen evolution. *Corros. Sci.* **2017**, *128*, 253–264. [[CrossRef](#)]
9. Adekanmbi, I.; Mosher, C.Z.; Lu, H.H.; Riehle, M.; Kubba, H.; Tanner, K.E. Mechanical behavior of biodegradable AZ31 magnesium alloy after long term in vitro degradation. *Mater. Sci. Eng.* **2017**, *77*, 1135–1144. [[CrossRef](#)] [[PubMed](#)]
10. Amerstorfer, F.; Fischerauer, S.F.; Fischer, L.; Eichler, J.; Draxler, J.; Zitek, A.; Meischel, M.; Martinelli, E.; Kraus, T.; Hann, S.; et al. Long-term in vivo degradation behavior and near-implant distribution of resorbed elements for magnesium alloys WZ21 and ZX50. *Acta Biomater.* **2016**, *42*, 440–450. [[CrossRef](#)] [[PubMed](#)]
11. Thomas, S.; Medhekar, N.V.; Frankel, G.S.; Birbilis, N. Corrosion mechanism and hydrogen evolution on Mg. *Curr. Opin. Solid State Mater. Sci.* **2015**, *19*, 85–89. [[CrossRef](#)]
12. Agarwal, S.; Curtin, J.; Duffy, B.; Jaiswal, S. Biodegradable magnesium alloys for orthopaedic applications: A review on corrosion, biocompatibility and surface modifications. *Mater. Sci. Eng. C* **2016**, *68*, 948–963. [[CrossRef](#)] [[PubMed](#)]
13. Wang, Y.; Ouyang, Y.; He, Y.; Chen, D.; Jiang, Y.; Mao, L.; Niu, J.; Zhang, J.; Yuan, G. Biocompatibility of Mg–Nd–Zn–Zr alloy with rabbit blood. *Chin. Sci. Bull.* **2013**, *58*, 2903–2908. [[CrossRef](#)]
14. Zheng, Y. *Magnesium Alloys as Degradable Biomaterials*; CRC Press: Boca Raton, FL, USA, 2015.
15. Ding, W. Opportunities and challenges for the biodegradable magnesium alloys as next-generation biomaterials. *Regen. Biomater.* **2016**, *3*, 79–86. [[CrossRef](#)] [[PubMed](#)]
16. Myrissaa, A.; Martinellia, E.; Szakács, G.; Berger, L.; Eichler, J.; Fischerauer, S.F.; Kleinhans, C.; Hort, N.; Schäfer, U.; Weinberg, A.M. In vivo degradation of binary magnesium alloys—A long-term study. *BioNanoMaterials* **2016**, *17*, 121–130. [[CrossRef](#)]
17. Soujanya, G.K.; Hanas, T.; Chakrapani, V.Y.; Sunil, B.R.; Kumar, T.S. Electrospun nanofibrous polymer coated magnesium alloy for biodegradable implant applications. *Procedia Mater. Sci.* **2015**, *5*, 817–823. [[CrossRef](#)]
18. Zheng, Y.; Gu, X.; Witte, F. Biodegradable metals. *Mater. Sci. Eng. R* **2014**, *77*, 1–34. [[CrossRef](#)]
19. Wan, P.; Tan, L.; Yang, K. Surface modification on biodegradable magnesium alloys as orthopedic implant materials to improve the bio-adaptability: A review. *J. Mater. Sci. Technol.* **2016**, *32*, 827–834. [[CrossRef](#)]
20. Wu, G.; Wang, X.; Ding, K.; Zhou, Y.; Zeng, X. Corrosion behavior of Ti–Al–N/Ti–Al duplex coating on AZ31 magnesium alloy in NaCl aqueous solution. *Mater. Charact.* **2009**, *60*, 803–807. [[CrossRef](#)]
21. Hu, J.; Guan, S.; Zhang, C.; Ren, C.; Wen, C.; Zeng, Z.; Peng, L. Corrosion protection of AZ31 magnesium alloy by a TiO₂ coating prepared by LPD method. *Surf. Coat. Technol.* **2009**, *203*, 2017–2020. [[CrossRef](#)]
22. Liu, C.; Xin, Y.; Tian, X.; Chu, P. Corrosion behavior of AZ91 magnesium alloy treated by plasma immersion ion implantation and deposition in artificial physiological fluids. *Thin Solid Films* **2007**, *516*, 422–427. [[CrossRef](#)]
23. Li, L.; Gao, J.; Wang, Y. Evaluation of cyto-toxicity and corrosion behavior of alkali-heat-treated magnesium in simulated body fluid. *Surf. Coat. Technol.* **2004**, *185*, 92–98. [[CrossRef](#)]
24. Yanovska, A.; Kuznetsov, V.; Stanislavov, A.; Danilchenko, S.; Sukhodub, L. Calcium–phosphate coatings obtained biomimetically on magnesium substrates under low magnetic field. *Appl. Surf. Sci.* **2012**, *258*, 8577–8584. [[CrossRef](#)]
25. Song, Y.; Shan, D.; Han, E. Electrodeposition of hydroxyapatite coating on AZ91D magnesium alloy for biomaterial application. *Mater. Lett.* **2008**, *62*, 3276–3279. [[CrossRef](#)]
26. Xu, L.; Pan, F.; Yu, G.; Yang, L.; Zhang, E.; Yang, K. In vitro and in vivo evaluation of the surface bioactivity of a calcium phosphate coated magnesium alloy. *Biomaterials* **2009**, *30*, 1512–1523. [[CrossRef](#)] [[PubMed](#)]
27. Xu, L.; Zhang, E.; Yang, K. Phosphating treatment and corrosion properties of Mg–Mn–Zn alloy for biomedical application. *J. Mater. Sci. Mater. Med.* **2009**, *20*, 859–867. [[CrossRef](#)] [[PubMed](#)]

28. Yang, J.; Cui, F.; Yin, Q.; Zhang, Y.; Zhang, T.; Wang, X. Characterization and degradation study of calcium phosphate coating on magnesium alloy bone implant in vitro. *IEEE Trans. Plasma Sci.* **2009**, *37*, 1161–1168. [[CrossRef](#)]
29. Xue, M.; Yao, Y.; Ou, J.; Wang, F.; Qu, Y.; Li, W. Effect of surface roughness on electron work function of AZ31 Mg alloy and their correlation. *J. Alloy. Compd.* **2018**, *731*, 44–48. [[CrossRef](#)]
30. Mohan, C. *Buffers. A Guide for the Preparation and Use of Buffers in Biological Systems*; EMD Bioscience: San Diego, CA, USA, 2006.
31. Yanovska, A.; Kuznetsov, V.; Stanislavov, A.; Danilchenko, S.; Sukhodub, L. Synthesis and characterization of hydroxyapatite-based coatings for medical implants obtained on chemically modified Ti6Al4V substrates. *Surf. Coat. Technol.* **2011**, *205*, 5324–5329. [[CrossRef](#)]
32. Feng, Y.; Zhu, S.; Wang, L.; Chang, L.; Yan, B.; Song, X.; Guan, S. Characterization and corrosion property of nano-rod-like HA on fluoride coating supported on Mg–Zn–Ca alloy. *Bioact. Mater.* **2017**, *2*, 63–70. [[CrossRef](#)] [[PubMed](#)]
33. Bai, N.; Tan, C.; Li, Q.; Xi, Z. Study on the corrosion resistance and anti-infection of modified magnesium alloy. *J. Biomed. Mater. Res. A* **2017**, *105*, 2750–2761. [[CrossRef](#)] [[PubMed](#)]
34. Zhang, M.; Cai, S.; Zhang, F.; Xu, G.; Wang, F.; Yu, N.; Wu, X. Preparation and corrosion resistance of magnesium phytic acid/hydroxyapatite composite coatings on biodegradable AZ31 magnesium alloy. *J. Mater. Sci. Mater. Med.* **2017**, *28*, 82. [[CrossRef](#)] [[PubMed](#)]
35. Xin, Y.; Hu, T.; Chu, P.K. In vitro studies of biomedical magnesium alloys in a simulated physiological environment: A review. *Acta Biomater.* **2011**, *7*, 1452–1459. [[CrossRef](#)] [[PubMed](#)]
36. Yu, Y.; Lu, H.; Sun, J. Long-term in vivo evolution of high-purity Mg screw degradation—Local and systemic effects of Mg degradation products. *Acta Biomater.* **2018**, *71*, 215–224. [[CrossRef](#)] [[PubMed](#)]
37. Grogan, J.A.; Brien, B.J.; Leen, S.B.; McHugh, P.E. A corrosion model for bioabsorbable metallic stents. *Acta Biomater.* **2011**, *7*, 3523–3533. [[CrossRef](#)] [[PubMed](#)]
38. Walker, J.; Shadanbaz, S.; Woodfield, T.B.; Staiger, M.P.; Dias, G.J. The in vitro and in vivo evaluation of the biocompatibility of Mg alloys. *Biomed. Mater.* **2014**, *9*, 015006. [[CrossRef](#)] [[PubMed](#)]
39. Jo, J.H.; Li, Y.; Kim, S.M.; Kim, H.E.; Koh, Y.H. Hydroxyapatite/poly(e-caprolactone) double coating on magnesium for enhanced corrosion resistance and coating flexibility. *J. Biomater. Appl.* **2012**, *28*, 617–625. [[CrossRef](#)] [[PubMed](#)]
40. Yang, H.; Xia, K.; Wang, T.; Niu, J.; Song, Y.; Xiong, Z.; Zheng, K.; Wei, S.; Lu, W. Growth, in vitro biodegradation and cytocompatibility properties of nano-hydroxyapatite coatings on biodegradable magnesium alloys. *J. Alloy. Compd.* **2016**, *672*, 366–373. [[CrossRef](#)]



© 2018 by the authors. Licensee MDPI, Basel, Switzerland. This article is an open access article distributed under the terms and conditions of the Creative Commons Attribution (CC BY) license (<http://creativecommons.org/licenses/by/4.0/>).